

## Localized spin ordering in Kondo lattice models

I. P. McCulloch,<sup>1</sup> A. Juozapavicius,<sup>2</sup> A. Rosengren,<sup>2</sup> and M. Gulacsi<sup>1</sup>

<sup>1</sup>*Department of Theoretical Physics, Institute of Advanced Studies, The Australian National University, Canberra, ACT 0200, Australia*

<sup>2</sup>*Department of Theoretical Physics, Royal Institute of Technology, SE-100 44 Stockholm, Sweden*

(Received 31 October 2001; published 10 January 2002)

Using a non-Abelian density matrix renormalization group method we determine the phase diagram of the Kondo lattice model in one dimension, by directly measuring the magnetization of the ground state. This allowed us to discover a second ferromagnetic phase missed in previous approaches. The phase transitions are found to be continuous. The spin-spin correlation function is studied in detail, and we determine in which regions the large and small Fermi surfaces dominate. The importance of double-exchange ordering and its competition with Kondo singlet formation is emphasized in understanding the complexity of the model.

DOI: 10.1103/PhysRevB.65.052410

PACS number(s): 75.30.Mb, 05.10.Cc, 71.10.Hf

The Kondo lattice model (KLM) describes the interaction between a conduction electron (CE) band and a half-filled narrow impurity, e.g.,  $f$  electron, band and is thought to capture the essential physics of the rare earth compounds. Although intensively studied for two decades, the KLM is still far from being completely understood. Recently, after the discovery of Kondo insulators and the non-Fermi-liquid behavior, interest in this field has been greatly renewed, especially due to the non-Fermi-liquid behavior discovered in most of the heavy fermion compounds, which resembles a Griffiths phase.<sup>1</sup>

In order to understand the role of the impurity spin in determining the properties of KLM we must develop a better understanding of the magnetic correlations. The Griffiths phase in the one-dimensional KLM occurs naturally;<sup>2</sup> it is, therefore, the prototypical model for heavy fermion compounds. Hence, this is an ideal system to study since we have the bosonized solution<sup>2,3</sup> and we know the behavior of the CE's in both the paramagnetic (PM) and ferromagnetic (FM) phases. However, less attention has been given to understand the correlations between the impurity spins. This is the focus of our study.

The Hamiltonian for the KLM is

$$H = -t \sum_{j=1, \sigma}^{L-1} (c_{j, \sigma}^\dagger c_{j+1, \sigma} + \text{H.c.}) + J \sum_{j=1}^L \mathbf{S}_j^c \cdot \mathbf{S}_j, \quad (1)$$

where  $t > 0$  is the CE hopping parameter,  $\mathbf{S}_j$  are spin 1/2 operators for the localized spins, e.g.,  $f$ , and  $\mathbf{S}_j^c = \frac{1}{2} \sum_{\sigma, \sigma'} c_{j, \sigma}^\dagger \boldsymbol{\sigma}_{\sigma, \sigma'} c_{j, \sigma'}$  with  $\boldsymbol{\sigma}$  the Pauli spin matrices and  $c_{j, \sigma}$ ,  $c_{j, \sigma}^\dagger$  the electron annihilation and creation site operators. The Kondo coupling  $J$  is measured in units of the hopping  $t$  and partial conduction band filling,  $n = N/L < 1$ , is assumed throughout.

The method that we use is density matrix renormalization group (DMRG) which, however, is extended to explicitly preserve SU(2) spin and pseudospin symmetry. Hence we can measure the magnetization directly and determine rigorously the PM-FM phase boundary. The obtained result is in excellent agreement with a recent bosonized solution<sup>2</sup> and contradicts the common view that this phase boundary goes to infinite Kondo coupling  $J$  as the CE density approaches half-filling.<sup>4,5</sup> We also determine the regions of the phase

diagram where large and small Fermi surfaces are dominant, which has been a central issue for much of the research in this area for some years.

In addition, we have discovered a second FM region not seen before. For most dopings, this region of FM separates the regions of large and small Fermi surface. This most likely resolves the question as to the applicability of the Luttinger theorem to the KLM, shown by Yamanaka *et al.*,<sup>6</sup> since the Fermi points are not expected to remain constant across a phase transition.

To accelerate the computation, we make use of several operators that commute with the Hamiltonian,  $S^+, S^-, S^z, I^+, I^-, I^z$ , respectively the generators of the spin SU(2) and pseudospin SU(2) algebras.<sup>7</sup> Combined, the generators form the algebra SO(4). All of the states in our DMRG calculation transform as irreducible representations of this algebra. Since SO(4) is non-Abelian these representations have, in general, degree  $> 1$ , which implies that a single basis state in the SO(4) representation is equivalent to multiple states of the purely Abelian representation of most previous DMRG calculations. This is the origin of the dramatic performance improvements of the non-Abelian DMRG. The states are labeled by the eigenvalues of the Casimir operators of SO(4), which are  $S^2 = s(s+1)$  and  $I^2 = i(i+1)$ . Hence we can label all irreducible representations by  $[s, i]$ , which has degree  $(2s+1)(2i+1)$ . In this construction, a chemical potential would appear as a term in the Hamiltonian proportional to  $I^z$ , acting in an identical way a magnetic field coupled to  $S^z$ . Although the basis states in the calculation are eigenstates of  $S^2$  and  $I^2$ , rather than  $S^z$  and  $I^z$ , all these operators mutually commute so it is possible to simply replace  $S^z$  and  $I^z$  by the chosen eigenvalues in this case. A single site of the Kondo lattice contains just three such states. The simplest is the Kondo singlet state, transforming as the  $[0, 0]$  representation of degree 1. The Kondo triplet state transforms as the  $[1, 0]$  representation of degree 3, and encapsulates the three projections  $|\uparrow\uparrow\rangle$ ,  $\sqrt{1/2}(|\uparrow\downarrow\rangle + |\downarrow\uparrow\rangle)$ ,  $|\downarrow\downarrow\rangle$  in a single state. Here,  $\uparrow$  denotes localized  $f$ , and  $\downarrow$  the conduction electron spins, respectively. Finally, the holon state (actually, the tensor product of a holon and a  $f$  spin) transforms as the  $[1/2, 1/2]$  representation of degree 4 and has the projections  $|\uparrow 0\rangle$ ,  $|\downarrow 0\rangle$ ,  $|\uparrow\uparrow\downarrow\rangle$ ,  $|\downarrow\downarrow\downarrow\rangle$ . The

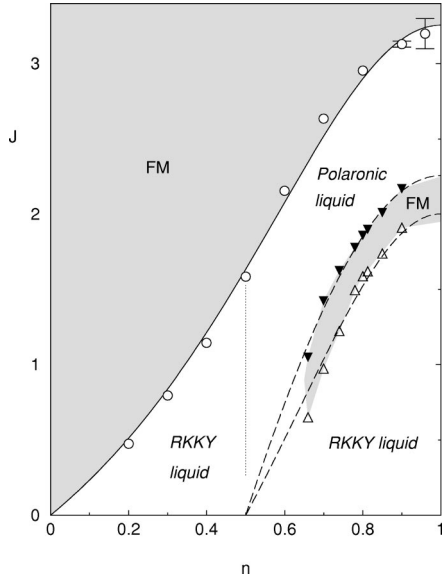


FIG. 1. The obtained phase diagram of KLM. The two shaded areas are the FM phases. The open circles and triangles correspond to points at which the FM energy level crosses the  $S=0$  level. The dashed curves are the derived phase transition lines (the solid curve was already obtained in Ref. 2).

single-site operators are  $3 \times 3$  matrices over this basis. The matrix elements can be determined by the Wigner-Eckart theorem, which specifies the relationship between the three-dimensional reduced basis and the full 8 dimensional basis. For a comprehensive description of the new algorithm, see Ref. 8. At half filling (where the ground state is a pseudospin singlet) 400 block states are equivalent to around 2500 states of a calculation using  $N$  and  $S^z$  quantum numbers, although the relative advantage of  $SO(4)$  decreases as the system is doped away from half filling. We used the new DMRG algorithm to obtain the ground state energy, magnetization, and different correlation functions, i.e., the momentum distribution, density-density, conduction electron spin-spin, and the  $f$  spin structure factor,  $S(k)$ . The obtained results can be summarized with the phase diagram presented in Fig. 1, which will be analyzed in detail hereafter. The main properties of the phase diagram have been confirmed on chains of 120 or more sites. Results for the magnetization were calculated on smaller chains, 40–60 sites, where the energies can be calculated more accurately. We found no finite size effects that would affect the properties of Fig. 1. In all cases, we extrapolate to zero truncation error based on well-converged sweeps of between 200 and 500  $SO(4)$  states kept.

As it can be seen from Fig. 1, the main feature dominating the KLM is  $f$  spin FM ordering. The FM ordering is due to the double-exchange (DE) interaction which appears as a consequence of an excess of localized spins over CE's:<sup>9</sup> each CE has to screen more than one localized spin, and since hopping is energetically most favorable for CE's that preserve their spin, this tends to align the localized spins. This element was missing in the early approaches, which concentrated on the competition between Kondo singlet formation at large  $J$  and the Ruderman-Kittel-Kasuya-Yosida (RKKY)

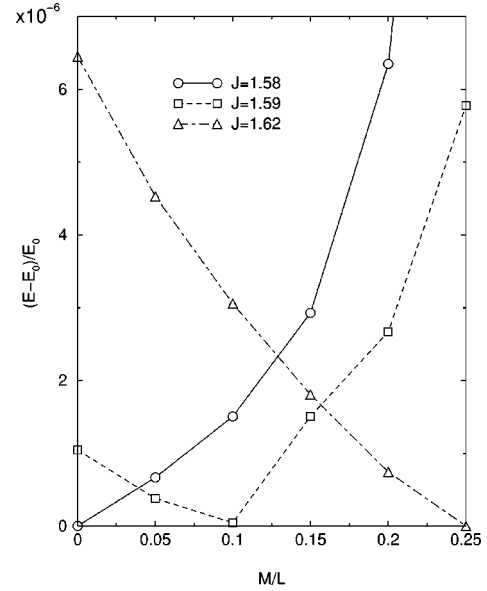


FIG. 2. Normalized magnetization curves (relative to the ground state energy,  $E_0$ ) across the phase transition at quarter filling for a 40 site lattice.

interaction in the weak coupling limit.<sup>10</sup> This picture is borrowed from the single-impurity Kondo model and is inadequate for the lattice case.<sup>4,5</sup>

Starting the analysis of the phase diagram for large  $J$ , we see that all CE's form singlets with the localized  $f$  spins<sup>11</sup> that become inert. The uncoupled  $f$  spins order FM in a mechanism similar to the  $J < 0$  case.<sup>9</sup> Here, there is no competition between Kondo singlet formation and DE. The fully polarized state [with  $S = (L - N)/2$ ] appears for any value of  $n < 1$ ,<sup>2,11</sup> contrary to the suggestion of Refs. 4 and 5 that close to half filling the PM phase extends to  $J \rightarrow \infty$ . As  $J$  is lowered, KLM can be rigorously mapped into a random transverse field Ising model;<sup>2</sup> hence the phase transition (the solid curve in Fig. 1) is identical to the quantum order-disorder transition. It should be emphasized that this is also true for the second FM phase, as will be shown later on.

The phase transition obtained via DMRG fits exceptionally well this picture, confirming the bosonization result of Ref. 2. The open circles correspond to points at which the energy of the FM state crosses the energy of the singlet state. Since the phase transition is second order, this is only an upper bound on the true transition line. However, the partially polarized region is very small, of the order of  $J/t \sim 0.01$ , which is why this phase transition has not previously been observed to be continuous. A typical example of the energy versus the magnetization ( $M$ ) is presented in Fig. 2. This shows that in the transition regime,  $\partial^2 E / \partial M^2$  is positive. We have accounted for all known random errors, these are errors arising from the tolerance of the matrix diagonalization, variations in the energy across the DMRG sweep, and error arising from the extrapolation to zero truncation error. These errors are of the order of the symbol size in this figure.

Below the solid curve, Fig. 1, the Kondo singlets are not inert anymore and they greatly contribute to the properties of

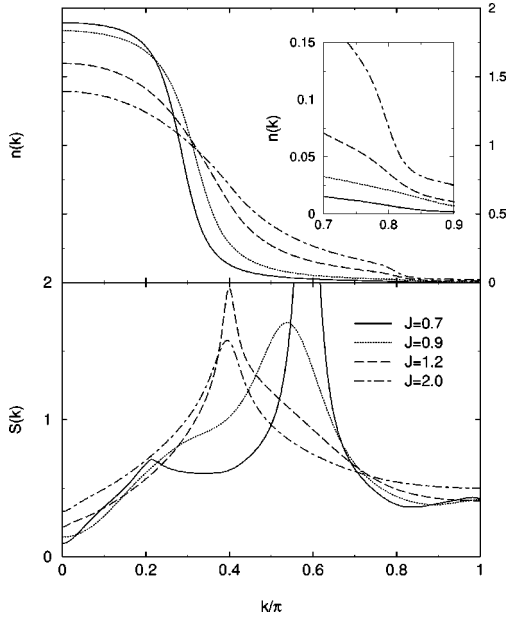


FIG. 3. Typical  $J$  dependence of the spin structure factor,  $S(k)$ , and the momentum distribution,  $n(k)$  ( $n=0.6$ ).

KLM. Excluding the Kondo triplet states, the CE wave function in the continuum limit satisfies a nonlinear Schrödinger equation<sup>12</sup> that has finitely delocalized solitonic solutions.<sup>13</sup> This corresponds to a dressing of the CE by a cloud of anti-parallel local spins, i.e., spin polarons are formed. The polaronic length scale competes with the length scale set by the free CE mean free path and introduces competing time scales: slow motion of the polarons with low energy dynamics and fast motion of the free CE's with high energies. This scenario resembles a two-fluid picture with intrinsic inhomogeneities which involves spin fluctuations and short-range spin correlations, which we call a *polaronic liquid*.

Finite temperature DMRG<sup>14</sup> confirmed the presence of short-range  $f$  spin correlations in the van Hove singularities. Consequently the structure factor peaks at  $2k_F - \pi$ , where  $k_F$  is the Fermi point determined by the filling of the CE band. This means that the localized  $f$  spins, even though they are completely immobile, contribute to the volume of the Fermi sea. This conventionally is called a *large* Fermi surface, the effect of which is also seen in the momentum distribution function (see Fig. 3). As the polarons are formed the peak of  $S(k)$  shifts from the small  $J/t$  value of  $2k_F$ : the slow motion of the spin polarons will dominate the low-energy dynamics of the quasiparticles. This proves that the appearance of the large Fermi surface is a dynamical effect since it involves local inhomogeneities, impurity spin fluctuation, and short-range correlations of the  $f$  spins. This phase is related<sup>2</sup> to a Griffiths phase, suggesting that the small to large Fermi surface crossover is a Griffiths singularity.

The large Fermi surface is conventionally explained by reference to the periodic Anderson model (PAM) ancestry.<sup>5,6,15</sup> Our results imply that even for PAM, this simple picture is inadequate. In particular, we see no reason why a small to large Fermi surface crossover, marked by a FM phase, should not also appear in PAM. However, the

behavior of the Fermi surface crossover close to quarter filling is numerically difficult to determine (dotted line in Fig. 1); hence we are not yet able to rule out the possibility that the large and small Fermi surface regions are adiabatically connected. Even prior to the current calculation, the nature of the Fermi surface in the weak-coupling regime was not clear, with the suggestion from Ref. 5 that the Fermi surface vanishes at a point in proximity to where we find the ferromagnetic phase. For  $n < 0.5$  the width of the polarons is over several lattice spacings [diverging for  $n \rightarrow 0$  (Ref. 12)] hence the energy needed to excite these polarons is too large for this effect to happen. The polarons will not contribute to the low-energy dynamics and the system behaves as an RKKY liquid, as we explain below.

An interesting phenomenon appears as we further lower  $J$ . The residual weight attached to the Kondo singlets vanishes; hence all CE's that participated in the formation of these singlets become delocalized. The distance between these CE's is much larger than the lattice spacing, and below  $J \leq 2\sqrt{n} \sin(\pi n)$  their continuum limit takes the regular quantum sine-Gordon form.<sup>3</sup> In the bosonization language of Ref. 2, this means that the spin Bose fields,  $\Phi_\sigma$  cannot be approximated by their noninteracting expectation values, rather by their expectation value corresponding to a sine-Gordon (sG) model,  $\Phi_\sigma \approx \langle \Phi_\sigma \rangle_{\text{sG}}$ . However, the charge degrees of freedom not being affected by the sine-Gordon spin gap, their corresponding Bose fields,  $\Phi_\rho$  may be still approximated by their noninteracting values. Extending the bosonized results of Ref. 2 to a finite  $\langle \Phi_\sigma \rangle_{\text{sG}}$ , we obtain the critical Hamiltonian governing the PM-FM phase transition at intermediate  $J$  values in the following form:  $H_{\text{crit}} = -[J^2 \mathcal{A} / (2\pi^2 v_F)] \sum_j \mathbf{S}_j^z \cdot \mathbf{S}_{j+1}^z + 2JB \sum_j \{1 - (\langle \Phi_\sigma \rangle_{\text{sG}}^2 / 2) [1 + J / (2\pi v_F)]^2 + \cos(2k_F j)\} \mathbf{S}_j^x$ , where  $\mathcal{A}$  and  $\mathcal{B}$  are functions that depend only on the cutoffs introduced by the bosonization scheme.<sup>2,3</sup> Following previous bosonization approaches closely,<sup>2,3</sup> we can prove that the critical behavior of the FM transition for the intermediate this  $J$  case is of a random transverse-field Ising model type, where the transverse field  $h_j = 2JB \{1 - (\langle \Phi_\sigma \rangle_{\text{sG}}^2 / 2) [1 + J / (2\pi v_F)]^2 + \cos(2k_F j)\}$  is driven by a displaced cosine distribution of the form  $\rho(h) = [1 / (2\pi JB)] (1 - \{h / (2JB) + (\langle \Phi_\sigma \rangle_{\text{sG}}^2 / 2) [1 + J / (2\pi v_F)]^2 - 1\}^2)^{-1/2}$ . Accordingly, the FM transitions emerging at intermediate values of  $J$  are of a quantum order-disorder type. These transitions are driven by spin polarons, contrary to the FM phase emerging at high  $J$  values, which is given by the uncoupled  $f$  spins (in a mechanism similar to the  $J < 0$  case). The new critical line is  $J_c = \alpha(\mathcal{A}, \mathcal{B}) \sin(\pi n / 2) / [1 - \beta(\mathcal{A}, \mathcal{B}) - \gamma(\mathcal{A}, \mathcal{B}, \langle \Phi_\sigma \rangle_{\text{sG}}^2)]$ . The bosonization (conformal field-theory) arguments do not determine the magnitude of  $\alpha$ ,  $\beta$ , and  $\gamma$ ; accordingly these constants are used as fitting parameters to the numerically obtained points. The best fits are the dashed curves in Fig. 1.

This is the second FM phase in Fig. 1, which has proven difficult to detect with conventional (Abelian) DMRG.<sup>16,17</sup> Previous DMRG calculations did show a weak FM signal at  $n=0.8$  and  $J=1.6$  and  $1.8$ ,<sup>15</sup> but the results were discarded in later papers by the same authors.<sup>5,4</sup> Likewise an exact diagonalization of a very small system gave FM for  $n$

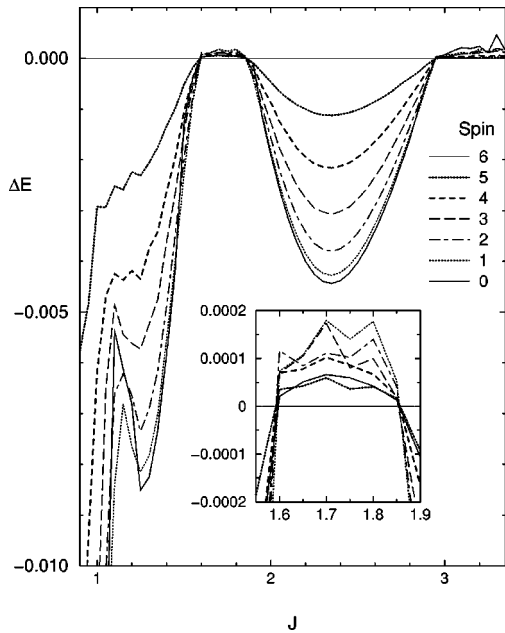


FIG. 4. The gap,  $\Delta E$ , from the fully polarized ferromagnetic state to every other spin state vs  $J$ , for  $n=0.8$  and a 60-site lattice, measured along intervals of  $J \pm 0.05$ . For most data points the error bars are of order  $\sigma_{\Delta E} \sim 10^{-5}$  or less, except for the  $S=0$  curve for very low and very high  $J$ , where the errors are of order  $\sigma_{\Delta E} \sim 5 \times 10^{-4}$ . The inset shows the second ferromagnetic region.

$=0.75$  and  $J=1.5$ .<sup>16</sup> Using the non-Abelian DMRG algorithm we could also check the energy of each total spin state, shown in Fig. 4, which clearly shows a second ferromagnetic region although we have not yet confirmed numerically the order of the phase boundaries. For the FM Kondo lattice

model,  $J < 0$ , a phase separated regime was observed in numerical approaches.<sup>18</sup> However, for  $J > 0$  we found no change in sign of the inverse charge compressibility. Thus, this phase is a true FM rather than a phase separated region.

Below the second FM region the KLM reduces to a system of free localized spins in fields determined by CE scattering: dominant  $2k_F$  modulations are manifest (see Fig. 3), superimposed on an incoherent background. This reflects the momentum transferred from the CE band to the spin chain in backscattering interactions, together with incoherent forward scattering. This case is referred to as an RKKY liquid as the scattering processes give an RKKY-like correlation for the  $f$  spins, even though the RKKY interaction strictly diverges in one dimension.

In conclusion, using a non-Abelian DMRG method a most comprehensive analysis of the short- and long-range ordering of the localized moments in KLM is presented. We show that DE ordering and its competition with Kondo singlet formation is the dominant feature of the phase diagram. The non-Abelian DMRG method allowed us to discover that FM does not only appear at large  $J$  but also at intermediate values. This second FM phase was missed in previous approaches. We also show that at large  $J$  FM is due to ordering of uncoupled  $f$  spins, while for intermediate  $J$ , i.e., the second FM region, FM is due to ordering of the spin polarons. The inhomogeneous polaronic state between these two FM phases is analogous to a two-fluid system and it exhibits a large Fermi surface.

The work in Australia was supported by the Australian Research Council and in Sweden by the Swedish Natural Science Research Council and The Swedish Foundation for International Cooperation in Research and Higher Education, STINT.

<sup>1</sup>M.C. de Andrade *et al.*, Phys. Rev. Lett. **81**, 5620 (1998).

<sup>2</sup>G. Honner and M. Gulacsi, Phys. Rev. Lett. **78**, 2180 (1997); Phys. Rev. B **58**, 2662 (1998).

<sup>3</sup>O. Zachar, S.A. Kivelson, and V.J. Emery, Phys. Rev. Lett. **77**, 1342 (1996).

<sup>4</sup>H. Tsunetsugu, M. Sigrist, and K. Ueda, Rev. Mod. Phys. **69**, 809 (1997).

<sup>5</sup>N. Shibata and K. Ueda, J. Phys.: Condens. Matter **11**, R1 (1999).

<sup>6</sup>M. Yamanaka, M. Oshikawa, and I. Affleck, Phys. Rev. Lett. **79**, 1110 (1997).

<sup>7</sup>B.A. Jones, C.M. Varma, and J.W. Wilkins, Phys. Rev. Lett. **61**, 125 (1988); T. Nishino and K. Ueda, Phys. Rev. B **47**, 12451 (1993).

<sup>8</sup>I.P. McCulloch and M. Gulacsi, cond-mat/0012319 (unpublished).

<sup>9</sup>C. Zener, Phys. Rev. **82**, 403 (1951); P.W. Anderson and H. Hasegawa, *ibid.* **100**, 675 (1955).

<sup>10</sup>R. Jullien, J.N. Fields, and S. Doniach, Phys. Rev. B **16**, 4889

(1977).

<sup>11</sup>M. Sigrist, H. Tsunetsugu, K. Ueda, and T.M. Rice, Phys. Rev. B **46**, 13838 (1992).

<sup>12</sup>M. Sigrist, H. Tsunetsugu, and K. Ueda, Phys. Rev. Lett. **67**, 2211 (1991).

<sup>13</sup>T. Holstein, Ann. Phys. (N.Y.) **16**, 407 (1961).

<sup>14</sup>N. Shibata and H. Tsunetsugu, J. Phys. Soc. Jpn. **68**, 3138 (1999).

<sup>15</sup>N. Shibata, K. Ueda, T. Nishino, and C. Ishii, Phys. Rev. B **54**, 13495 (1996).

<sup>16</sup>H. Tsunetsugu, M. Sigrist, and K. Ueda, Phys. Rev. B **47**, 8345 (1993).

<sup>17</sup>M. Troyer and D. Würtz, Phys. Rev. B **47**, 2886 (1993); S. Moukouri and L.G. Caron, *ibid.* **52**, R15 723 (1995); S. Caprara and A. Rosengren, Europhys. Lett. **39**, 55 (1997); I.P. McCulloch, M. Gulacsi, S. Caprara, A. Juozapavicius, and A. Rosengren, J. Low Temp. Phys. **117**, 323 (1999).

<sup>18</sup>S. Yunoki *et al.*, Phys. Rev. Lett. **80**, 845 (1998); E. Dagotto *et al.*, Phys. Rev. B **58**, 6414 (1998).